

K. Lindfors, T. Kalkbrenner, P. Stoller, and V. Sandoghdar. 2004. Detection and spectroscopy of gold nanoparticles using supercontinuum white light confocal microscopy. *Physical Review Letters*, volume 93, number 3, 037401.

© 2004 American Physical Society

Reprinted with permission.

Readers may view, browse, and/or download material for temporary copying purposes only, provided these uses are for noncommercial personal purposes. Except as provided by law, this material may not be further reproduced, distributed, transmitted, modified, adapted, performed, displayed, published, or sold in whole or part, without prior written permission from the American Physical Society.

<http://link.aps.org/abstract/prl/v93/e037401>

Detection and Spectroscopy of Gold Nanoparticles Using Supercontinuum White Light Confocal Microscopy

K. Lindfors,* T. Kalkbrenner,[†] P. Stoller, and V. Sandoghdar[‡]

Laboratory of Physical Chemistry, Swiss Federal Institute of Technology (ETH), CH-8093 Zurich, Switzerland

(Received 26 November 2003; published 15 July 2004)

We combine confocal microscopy using supercontinuum laser illumination and an interferometric detection technique to identify single nanoparticles of diameter below 10 nm. Spectral analysis of the signal allows us to record the plasmon resonance of a single nanoparticle. Our results hold great promise for fundamental studies of the optical properties of single metal clusters and for their use in biophysical applications.

DOI: 10.1103/PhysRevLett.93.037401

PACS numbers: 78.67.Bf, 73.20.Mf, 78.35.+c, 87.64.Tt

Plasmon resonances in metallic nanoparticles are due to the collective oscillation of conduction electrons against their matrix. These resonances play a central role in the optical properties of metallic nanoparticles and have fascinated scientists for a long time [1,2]. Recently the progress in nanosciences has fueled a new wave of investigations on metallic nanoparticles, encompassing fabrication [3–5] and theoretical modeling of their optical properties [6–8]. A wide range of new applications such as subwavelength architectures for integrated optics [9], scanning near-field optical microscopy (SNOM) [10], and biological labeling [11,12] has also been discussed. The realization of many of these ideas, however, requires reliable and convenient methods for optical detection and characterization of metallic nanoparticles. In particular, for applications such as labeling and for fundamental studies such as spectroscopy, it is desirable to push the limits of detection to ever decreasing particle size.

Although experiments with single fluorescent molecules have become routine in the laboratory [13], detection of single metallic nanoparticles as small as a few nanometers is regarded as a challenge [14]. One reason is that while Stokes shifted emission of a molecule can be spectrally filtered from the background excitation light, distinguishing the elastically scattered light of a nanoparticle from the background is not trivial. Several methods such as SNOM [15], dark-field microscopy [12], and total internal reflection imaging [16] have been employed to achieve this goal in the past few years. However, it has not been possible to detect very small particles because the scattering signal from a particle of diameter D scales as D^6 , so that it rapidly vanishes below the background level as D is decreased. Very recently a clever implementation of the photothermal effect has overcome this scaling law by detecting a nanoparticle via its absorption cross section, which varies as D^3 [14]. Given these recent endeavors, it is surprising that as early as 1986 scientists from the biophysics community have claimed that the scattered light from particles down to 5 nm can be detected in video microscopy [17]. In this Letter we report

on the optical detection of single gold nanoparticles smaller than 10 nm by using an interferometric scheme very similar to that proposed by Batchelder and Taubenblatt [18] and used in near-field experiments [19,20]. We present a simple model that agrees with our experimental results and clarifies some of the observations reported in the literature. Furthermore, we present the first plasmon spectra of such tiny individual particles.

In our experiment we illuminate the sample with supercontinuum laser light generated in a photonic crystal fiber (PCF) through a cascade of nonlinear effects that give rise to a spectrum extending from the visible to the near infrared [21]. An example is given in Fig. 1(a). A picosecond Ti:sapphire laser beam (Coherent Mira) at

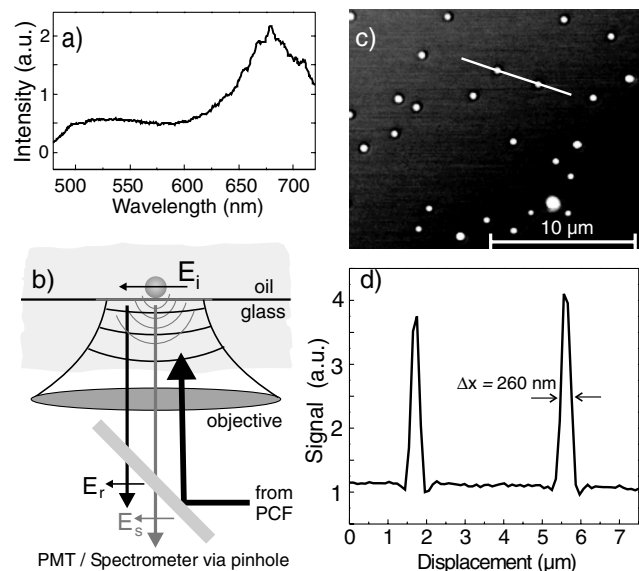


FIG. 1. (a) A spectrum of the supercontinuum white-light laser source. (b) Schematics of the experimental arrangement illustrating the interaction between a gold nanoparticle and the optical field. (c) A white-light confocal scan of a sample containing 60 nm particles. (d) Cross section marked in (c), showing that the supercontinuum light beam can be tightly focused.

$\lambda = 775$ nm was coupled into the PCF with a core diameter of about $2 \mu\text{m}$, and an electro-optical modulator was placed before the PCF to stabilize its output.

The central part of the experimental arrangement is shown in Fig. 1(b). The samples were prepared by spin coating a dilute solution of gold nanoparticles (British Biocell) onto a microscope cover glass. A drop of immersion oil was added to nearly match the index of the substrate [22], providing a homogeneous optical medium. The supercontinuum laser beam with a typical power of about 1 mW [23] was focused onto the sample using a microscope objective of a high numerical aperture and a high degree of chromatic correction. A piezoelectric element was used to raster scan the sample in the focus of the microscope objective. The optical signal was collected in reflection, passed through a pinhole and sent to a photomultiplier (PMT) or to a spectrometer equipped with a nitrogen-cooled charge-coupled device camera.

Let E_i denote the electric field of the incident laser beam seen by the sample in the focus of the microscope objective [see Fig. 1(b)]. The incident field undergoes reflection at the interface between glass and immersion oil, giving rise to the field $E_r = rE_i e^{-i\pi/2}$ at the detector. Here the real quantity r takes into account an effective field reflectivity for the focused beam. The field does not experience a phase shift upon reflection from a medium of lower refractive index [22], but a phase of $-\pi/2$ has been introduced to account for the Gouy phase shift [24] that is accumulated by the reflected Gaussian beam with respect to E_i . We note that although the reflection of a tightly focused beam could have a complicated character, this is not the case for our index-matched system [25].

For a spherical nanoparticle of diameter $D \ll \lambda$ the scattered light propagates as a spherical wave, is collimated by the microscope objective, and interferes with E_r . The scattered field at the detector can be written as $E_s = sE_i$, where $s = |s|e^{i\varphi}$ is proportional to the polarizability α of the particle [26],

$$s(\lambda) = \eta\alpha(\lambda) = \eta\epsilon_{\text{med}}(\lambda) \frac{\pi D^3}{2} \frac{\epsilon_{\text{part}}(\lambda) - \epsilon_{\text{med}}(\lambda)}{\epsilon_{\text{part}}(\lambda) + 2\epsilon_{\text{med}}(\lambda)}. \quad (1)$$

Here η takes into account the detection efficiency while $\epsilon_{\text{part}}(\lambda)$ and $\epsilon_{\text{med}}(\lambda)$ are the complex dielectric constants of the particle and the medium, respectively. The measured intensity I_m at the detector is then written as

$$I_m = |E_r + E_s|^2 = |E_i|^2 \{r^2 + |s|^2 - 2r|s| \sin\varphi\}. \quad (2)$$

The term proportional to r^2 is simply the background intensity which in our confocal detection scheme almost entirely originates from the interface between the sample's upper surface and the immersion oil. The term proportional to $|s|^2$ is the pure scattering signal which drops as D^6 . The last term in Eq. (2), on the other hand, scales as D^3 and therefore does not drop as fast. Figure 1(c) shows the photomultiplier signal from a confocal scan of a sample containing 60 nm particles, and

Fig. 1(d) displays a cross section through this image. Here the second term dominates so that the particles appear brighter than the background, as in the case of common detection schemes [12,16]. As the particle size decreases, the last term in Eq. (2) becomes more important. In addition, because this cross term is multiplied by the field reflectivity r , it overwhelms the pure scattering contribution for very small particles. As a result, we have been able to detect single gold particles down to a nominal diameter of $D = 5$ nm, discussed in more detail later.

Besides a high detection sensitivity, an important aspect of our work is to perform spectroscopy on individual gold nanoparticles. To do this we direct the detected light to the spectrometer and record spectra at each scan pixel. In order to account for the spectral characteristics of the incident laser beam and any wavelength dependence inherent in the setup, we normalize each measured spectrum to a reference spectrum $I_r(\lambda) = |E_r(\lambda)|^2$ recorded next to the particle. Using Eqs. (1) and (2) we obtain

$$\begin{aligned} \sigma(\lambda) &= \frac{I_m(\lambda) - I_r(\lambda)}{I_r(\lambda)} \\ &= \frac{\eta^2}{r^2} |\alpha(\lambda)|^2 - 2\frac{\eta}{r} |\alpha(\lambda)| \sin[\varphi(\lambda)]. \end{aligned} \quad (3)$$

Figures 2(a)–2(e) plot $\sigma(\lambda)$ measured for single particles of nominal diameter 60, 30, 20, 10, and 5 nm, respectively. For the case of a 60 nm particle the first term in Eq. (3) dominates so that the spectrum resembles a familiar plasmon resonance. For a 30 nm particle the two terms compete, yielding a pronounced dispersive character, while for smaller particles the second term

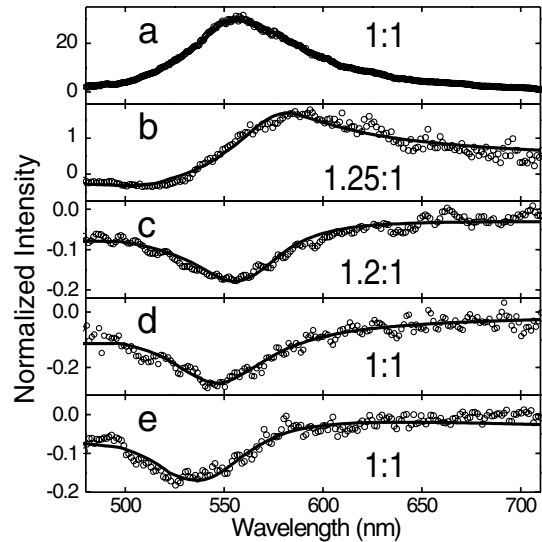


FIG. 2. Normalized plasmon spectra of single gold nanoparticles of various diameters (as specified by the manufacturer): (a) 60 ± 12 nm, (b) 31 ± 6 nm, (c) 20 ± 4 nm, (d) 10.3 ± 1.0 nm, and (e) 5.4 ± 0.8 nm. The symbols show the experimental data while the solid curves are fits that consider spheroidal particles. The fit outcome for the ratio of the spheroid axes $a:b$ is shown in the legend of each figure.

dominates, and the resonance profile becomes purely absorptive. The solid curves in Fig. 2 display the fits to the spectra using the bulk values of the complex dielectric constant of gold [27] to calculate $\alpha(\lambda)$, allowing for a small degree of ellipticity in the plane of the substrate [26]. We note very good agreement with the experimental data. Since the index of the glass substrate is nearly matched by that of oil, we can avoid the difficulties associated with the influence of interfaces on the plasmon spectra [28].

In order to gain more insight into the underlying mechanism of our detection scheme, in Fig. 3 we plot the normalized signal $\frac{1}{(\lambda_1 - \lambda_2)} \int \sigma(\lambda) d\lambda$ averaged over the wavelength range 480–700 nm for particles of nominal diameter 60, 30, 20, 15, 10, and 5 nm. Symbols represent the experimental data. The solid curve shows a fit to the data obtained by integrating over the theoretically expected $\sigma(\lambda)$ for spherical particles, where η/r in Eq. (3) was left as a free fit parameter. The data in Fig. 3 elucidate the contrast reversal encountered in the spectra of Fig. 2 and show that the dependence of the measured signal on the particle size follows a nontrivial trend. In light of our findings we believe the detection sensitivity and contrast reported from work in video microscopy [17] is due to the cross term and possibly absorption and not to the pure scattering contribution.

The agreement between the experimental data and the theoretical fit in Fig. 3 is very good over 3 orders of magnitude, giving a robust proof that we have detected single particles in each experiment. The contrast obtained from the nominal 5 nm particles is, however, larger than expected. The first thought might be that we have systematically detected agglomerates of particles. Another possibility is that the particles are slightly larger than specified by the manufacturer. An indication that we do not detect our signal from many particles is displayed in Figs. 4(a) and 4(b) where confocal and atomic force

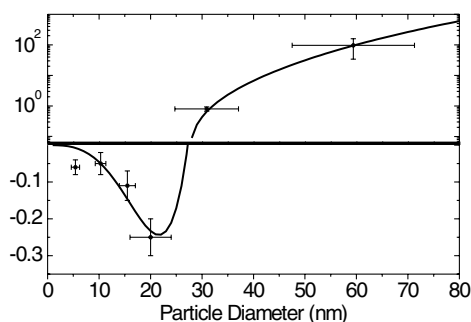


FIG. 3. Normalized signal σ from nanoparticles of various sizes averaged over the wavelength region of 480–700 nm. Because of the large signal dynamics, we have plotted the positive values on a logarithmic axis, and the negative values linearly. The horizontal error bars show the uncertainty in the particle diameter as specified by the manufacturer. The vertical bars were determined from the spread in σ measured for several tens of particles. See the text for details.

037401-3

microscope (AFM) images of the same sample area show a nearly one-to-one correspondence. Although the limited lateral resolution of AFM (~ 40 nm) does not allow us to rule out very small aggregates, the measured heights of the spots in the AFM image are all consistent with those of single particles. To shed more light on this issue we present the signal from more than 110 particles in the histogram of Fig. 4(c). The histogram has a spread of about a factor of 2. This spread is also illustrated in Fig. 4(d) where two cross sections of the confocal image are presented. While some particles (see curve *ii*) are detected with a good signal-to-noise ratio (SNR), others (see curve *i*) are barely visible. We believe that both the higher observed optical contrast and the spread in it are caused by the deviation of the particle size from the average value specified by the manufacturer. To investigate this we have performed high-resolution transmission electron microscopy and have verified that, indeed, the particles range between 8 and 5 nm in size. The corresponding decrease in the optical contrast by up to a factor of 4 can drown the signal in the noise [see Fig. 4(d)]. In other words, in recording the spectra we have systematically favored particles with larger signals, leading to an anomaly in the last data point of Fig. 3.

We now remark on the signal-to-noise ratio in our detection scheme. Let us consider Eq. (2). The first term denotes a constant background I_r , which can be subtracted from the measured signal. However, the noise δI_r , associated with this quantity persists. For very small particles we can neglect the second term so that the SNR of the measurement depends only on the size of the cross term $2|E_i|^2 r |s| \sin \phi$ relative to δI_r . In our current experiment

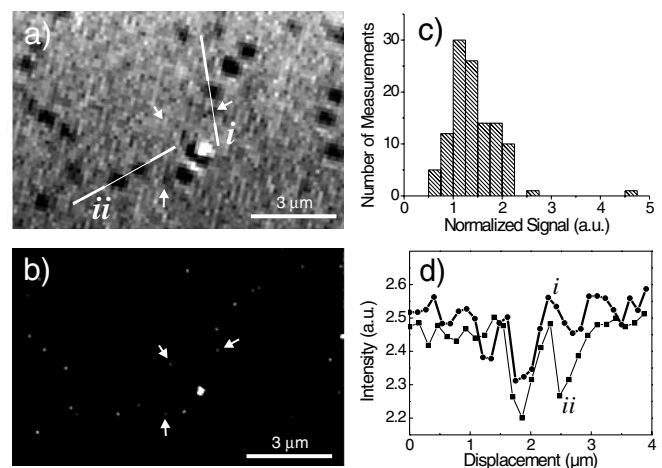


FIG. 4. (a) A raw confocal image of a sample containing nominal 5 nm nanoparticles. (b) An AFM image of the same area. Three arrows in (a) and (b) point to a particle that is missing in the optical image and to two others that give very weak signals. An area of small aggregation or dirt is also seen in both images (a) and (b). (c) A histogram of the signal strength from more than 110 particles with a nominal diameter of 5 nm. (d) Cross sections marked in (a) show the variation of SNR.

037401-3

we have been limited by the intensity noise of the supercontinuum light, but in the ideal situation of a shot-noise limited beam δI_r scales with r , and the SNR becomes independent of this parameter. In other words, in this limit the SNR does not depend on the intensity of the incident light. This feature has a crucial advantage in studying fast dynamic processes in biophysical applications because one can reduce the signal integration times and still collect enough photons by increasing the incident laser intensity. We note in passing that the detection scheme presented here can also use monochromatic light if one is not interested in recording plasmon spectra. However, spectral information is very valuable for identifying the signal of a metallic nanoparticle from other scatterers such as constituents of a biological system. This can be achieved by modulating the illumination wavelength at the side of the plasmon resonance and implementing a synchronous detection scheme.

In conclusion, we have succeeded in detecting individual gold nanoparticles below 10 nm using a fully optical technique. Furthermore, by using a focusable supercontinuum white-light source, we have recorded for the first time plasmon spectra of these particles. One of the most promising applications of our detection technique is *in vivo* single particle tracking and localization [29] as well as sensing [30] in biophysical applications. Gold nanoparticles neither photobleach nor blink and are small enough so as not to inhibit penetration or diffusion in most biological systems. Furthermore, by varying the phase between an external reference field E_r and the scattered field E_s , we plan to extract the real and imaginary parts of the scattered field [31] and of the dielectric constant as a function of wavelength.

We are grateful to L. Rogobete, B. Lounis, and C. Hettich for fruitful discussions. We are indebted to J. Knight (University of Bath) for the generous supply of PCFs and thank M. Müller for support in electron microscopy. K.L. acknowledges support from the Finnish Graduate School of Modern Optics and Photonics and the Vilho, Yrjö, and Kalle Väisälä, Tekniikan edistämissäätiö, Ella and Georg Ehrnrooth foundations. This work was financed by ETH Zurich.

*Permanent address: Department of Engineering Physics and Mathematics, Helsinki University of Technology, P.O. Box 2200, FIN-02015 HUT, Finland.

†Current address: FOM Institute for Atomic and Molecular Physics, Kruislaan 407, 1098 SJ Amsterdam, The Netherlands.

‡Electronic addresses: vahid.sandoghdar@ethz.ch
http://www.nano-optics.ethz.ch

[1] M. Kerker, *J. Colloid Interface Sci.* **105**, 297 (1985).

- [2] U. Kreibig and M. Vollmer, *Optical Properties of Metal Clusters*, Springer Series in Materials Science Vol. 25 (Springer, Berlin, New York, 1995).
- [3] Y. Sun and Y. Xia, *Science* **298**, 2176 (2002).
- [4] J. Aizpurua *et al.*, *Phys. Rev. Lett.* **90**, 057401 (2003).
- [5] R. Jin *et al.*, *Nature (London)* **425**, 487 (2003).
- [6] M. Quinten, *Appl. Phys. B* **67**, 101 (1998).
- [7] J. P. Kottmann, O. J. F. Martin, D. R. Smith, and S. Schultz, *Phys. Rev. B* **64**, 235402 (2001).
- [8] E. Prodan, C. Radloff, N. J. Halas, and P. Nordlander, *Science* **302**, 419 (2003).
- [9] H. Ditlbacher, J. R. Krenn, G. Schider, A. Leitner, and F. R. Aussenegg, *Appl. Phys. Lett.* **81**, 1762 (2002).
- [10] T. Kalkbrenner, M. Ramstein, J. Mlynek, and V. Sandoghdar, *J. Microsc.* **202**, 72 (2001).
- [11] C. J. Cogswell, D. K. Hamilton, and C. J. R. Sheppard, *J. Microsc.* **165**, 103 (1992).
- [12] S. Schultz, D. R. Smith, J. J. Mock, and D. A. Schultz, *Proc. Natl. Acad. Sci. U.S.A.* **97**, 996 (2000).
- [13] *Single Molecule Spectroscopy*, edited by R. Rigler, M. Orrit, and T. Basche (Springer, New York, 2001).
- [14] D. Boyer, P. Tamarat, A. Maali, B. Lounis, and M. Orrit, *Science* **297**, 1160 (2002).
- [15] T. Klar *et al.*, *Phys. Rev. Lett.* **80**, 4249 (1998).
- [16] G. Sönnichsen *et al.*, *Appl. Phys. Lett.* **77**, 2949 (2000).
- [17] M. De Brabander, R. Nuydens, G. Geuens, M. Moeremans, and J. De Mey, *Cell Motil. Cytoskeleton* **6**, 105 (1986).
- [18] J. S. Batchelder and M. A. Taubenblatt, *Appl. Phys. Lett.* **55**, 215 (1989).
- [19] F. Zenhausern, M. P. O'Boyle, and H. K. Wickramasinghe, *Appl. Phys. Lett.* **65**, 1623 (1994).
- [20] A. A. Mikhailovsky, M. A. Petruska, M. I. Stockman, and V. I. Klimov, *Opt. Lett.* **28**, 1686 (2003).
- [21] J. K. Ranka, R. S. Windeler, and A. J. Stentz, *Opt. Lett.* **25**, 25 (2000).
- [22] The refractive indices of the immersion oil and the cover glass vary from $n = 1.524$ to $n = 1.512$ and $n = 1.523$ to $n = 1.513$, respectively, in the spectral domain of 500–700 nm.
- [23] Following the calculations of Ref. [14] this amount of light spread over a broad spectrum leads to a temperature increase of less than 0.5° at the particle surface.
- [24] B. E. A. Saleh and M. C. Teich, *Fundamentals of Photonics* (Wiley-Interscience, New York, 1991).
- [25] L. Novotny, R. D. Grober, and K. Karrai, *Opt. Lett.* **26**, 789 (2001).
- [26] C. F. Bohren and D. R. Huffman, *Absorption and Scattering of Light by Small Particles* (Wiley Interscience, New York, 1983).
- [27] P. B. Johnson and R. W. Christy, *Phys. Rev. B* **6**, 4370 (1972).
- [28] P. A. Bobbert and J. Vlieger, *Physica (Amsterdam)* **137A**, 209 (1986).
- [29] B. J. Schnapp, J. Gelles, and M. P. Sheetz, *Cell Motil. Cytoskeleton* **10**, 47 (1988).
- [30] R. Elghanian, J. J. Storhoff, R. C. Mucic, R. L. Letsinger, and C. A. Mirkin, *Science* **277**, 1078 (1997).
- [31] Y. Matsuo and K. Sasaki, *Jpn. J. Appl. Phys.* **40**, 6143 (2001).